Available online at www.sciencedirect.com
SCIENCE DIRECT
Journal of Hydrology 311 (2005) 230–243
Journal of Hydrology
www.elsevier.com/locate/jhydrol

Temporal changes in hydraulic conductivity of sand porous media biofilters during wastewater infiltration due to biomat formation

Deborah N.H. Beach[a], John E. McCray[b,*], Kathryn S. Lowe[b], Robert L. Siegrist[b]

[a]*Department of Geological and Mining Engineering and Sciences, Michigan Technological University, Houghton, MI 49931, USA*
[b]*Division of Environmental Engineering and Science, Colorado School of Mines, 1500 Illinois Street, Golden, CO 80401-1887, USA*

Received 27 March 2003; revised 11 January 2005; accepted 25 January 2005

Abstract

Porous media biofilters (PMBs) are commonly used to treat domestic wastewater. Biomats develop at the infiltrative surface of PMBs due to continued wastewater application and create an impedance to flow. The goal of this research is to quantify the temporal evolution of normalized biomat hydraulic conductivity (K_{bm}/b_{bm}) and effective hydraulic conductivity (K_e). K_e is the overall hydraulic conductivity of the infiltrative zone, including biomat and unsaturated media below the biomat. Research was conducted using eight one-dimensional (1D) sand columns with gravel-free and gravel-laden infiltrative surfaces. The columns were loaded at design rates of 100–200 cm/d for 20 weeks of column operation. The K_e values for these continuously loaded columns were determined from analyses of bromide-tracer tests, falling-head permeability tests, and volumetric water content measurements during biomat development. The reduction in the K_e due to biomat formation is due to two factors: reduced hydraulic conductivity of the thin biomat, and a reduced hydraulic conductivity of the subsoil due to development of a biomat-induced unsaturated flow regime. Unsaturated hydraulic conductivities of the subsoil below the biomat (K_{ss}) were estimated from capillary curves and water content measurements. For observed final biomat thicknesses (less than 1 cm), the biomat hydraulic conductivity, K_{bm}, is three orders of magnitude smaller than the unsaturated hydraulic conductivity (K_{ss}). However, the relatively large thickness of the vadose zone causes the K_{ss} to be an important contributor to the overall K_e value. For these columns, the final K_e values were approximately two orders of magnitude smaller than the original value. Because the exact thickness of the biomat (b_{bm}) is unknown during the flow experiments, the hydraulic conductance of the biomat zone is presented using a normalized hydraulic conductivity function (K_{bm}/b_{bm}). A similar K_{bm}/b_{bm} is reached regardless of wastewater loading rate. An exponential relationship exists between the volume of wastewater applied to the column and both K_e and K_{bm}/b_{bm}.

Keywords: Wastewater; Hydraulic conductivity; Infiltration; Porous media biofilters; Biomat

1. Introduction

Porous media biofilters (PMBs), also known as sand filters or soil absorption systems, are commonly used in the United States to treat and manage domestic

* Corresponding author. Tel.: +1 303 273 3490; fax: +1 303 273 3413.
E-mail addresses: dnbeach@mtu.edu (D.N.H. Beach), jmccray@mines.edu (J.E. McCray), klowe@mines.edu (K.S. Lowe), siegrist@mines.edu (R.L. Siegrist).

0022-1694/$ - see front matter © 2005 Elsevier B.V. All rights reserved.
doi:10.1016/j.jhydrol.2005.01.024

wastewater. Biomats develop at the infiltrative surface of a PMB as a result of continued wastewater application. The mechanisms of biomat development are not fully understood, although several studies have been completed in the attempt to characterize biomat formation in subsurface PMBs. According to the literature, the development of a biomat layer at or just below the infiltrative surface seems to result from both the accumulation of suspended solids within soil pores and microbiological growth (Jones and Taylor, 1965; Thomas et al., 1966; Bouma, 1975; Siegrist and Boyle, 1987; Tyler et al., 1991; Tyler and Converse, 1994).

The steady-state infiltration rate that a PMB can accept is controlled by four main factors: (1) the hydraulic conductivity of the infiltrative surface, including the biomat; (2) the height of ponding above the infiltrative surface; (3) the thickness of the biomat; (4) the moisture tension of the subsoil, which determines the unsaturated hydraulic conductivity for a particular soil (Hargett et al., 1981; Beach and McCray, 2003). Of these factors, the hydraulic conductivity of the biomat is the least understood and most difficult to quantify.

Biomat development creates an increased resistance to flow; and therefore strongly influences the unsaturated flow regime within a PMB. Unsaturated flow conditions are critical for effective purification of wastewater effluents, such as septic tank effluent (STE), by promoting contact between wastewater constituents and the surface of soil particles, thereby increasing the time available for treatment processes to occur (Schwager and Boller, 1997; Van Cuyk et al., 2001; Siegrist et al., 2001).

Unfortunately, there are few detailed hydraulic characterizations of the PMB during biomat development. Based on data and information in the literature, the formation of basal and sidewall biomats at the infiltrative surfaces of soil PMBs decreases the infiltration rate and effective hydraulic conductivity of the system (Jones and Taylor, 1965; Bouma, 1975; Siegrist, 1987; Siegrist and Boyle, 1987; Keys et al., 1998; Beach and McCray, 2003). Reductions in the overall 'effective' hydraulic conductivity of PMBs are due to decreases in the biomat conductivity, as well as decreases in the unsaturated conductivity that occur as the biomat forms.

The major objective of this research effort was to analyze the development of the biomat and the associated hydraulic performance for sand-filled columns (i.e. PMBs) under different hydraulic loading conditions and with different infiltration surface architectures (with and without gravel). Hydraulic results were obtained from several independent laboratory measurements conducted prior to wastewater application, during wastewater application and biomat formation, and after final quasi-steady-state hydraulic conditions were reached. These measurements include: time domain reflectometry (TDR) derived water contents, bromide tracer tests, daily volumetric flow rates of the column effluent (also called 'throughput rates'), and falling head infiltration rates. From this data, biomat-induced temporal variations in hydraulic conductivity of continuously loaded columns were estimated. A discussion of hydraulic behavior and biological treatment of all columns based on effluent throughput rates is forthcoming (Lowe et al., submitted for publication).

2. Methods

2.1. Experimental apparatus and application

To determine the effects of different loading rates on hydraulic performance, sixteen (16), 1D columns were created to simulate a vertical slice within a PMB under four loading regimes. The experimental design conditions for each column are described in Table 1. There are many methods of wastewater dispersal for systems serving single-family homes, as well as clusters of homes and commercial establishments. A typical field application rate of domestic STE to a sandy PMB is 5 cm/d (Siegrist et al., 2001). The design rates for each loading regime in this study were chosen to represent four possible field conditions during startup and maturation and are summarized in Table 1. Due to biomat development and operational factors during column operation, the actual hydraulic loading rates to the columns and throughput rates were less than their design rates as the experiment progressed. Based on volume of wastewater processed, the higher loading rates (Table 1) for 20 weeks of column operation reflect equivalent times of operation up to 15.4 years for a home if all wastewater applied was accepted (e.g. 200 cm/d for 20 weeks equals 5 cm/d for 15.4 years).

Table 1
Loading regimes and experimental design conditions for column lysimeters

Loading regime	Column labels	Infiltrative surface architecture	Representative field condition	Application method	Dosing rate	Experimental design hydraulic loading rate[a]
LR1	1A, 1B 1C, 1D	Gravel-free Gravel-laden	Random gravity distribution in a serial trench network	Continuous delivery	24.56 mL/min continuous	200 cm/d, 35.36 L/d
LR2	2A, 2B 2C, 2D	Gravel-free Gravel-laden	Random gravity distribution in a trench network		12.28 mL/min continuous	100 cm/d, 17.68 L/d
LR3	3A, 3B 3C, 3D	Gravel-free Gravel-laden	Dosed, non-uniform distribution between orifices	Four equal doses per day at 8, 12, 16, and 20 (out of 24 h)	1.10 L/min for 2 min	50 cm/d, 8.84 L/d
LR4	4A, 4B 4C, 4D	Gravel-free Gravel-laden	Dosed, uniform distribution between orifices		1.10 L/min for 1 min	25 cm/d, 4.42 L/d

[a] Actual initial loading rates were approximately 85–95% of the experimental design due to operational factors described in the text.

The columns were constructed from clear acrylic pipe, 15 cm in diameter (surface area = 176.7 cm^2) and 105 cm in length (Fig. 1). Outflow and overflow ports were tapped near the bottom and top of each column, with the overflows positioned approximately 20 cm above the infiltrative surface. Prior to packing with sand, the inside walls of the column were sprayed with an acrylic adhesive and covered with sand.

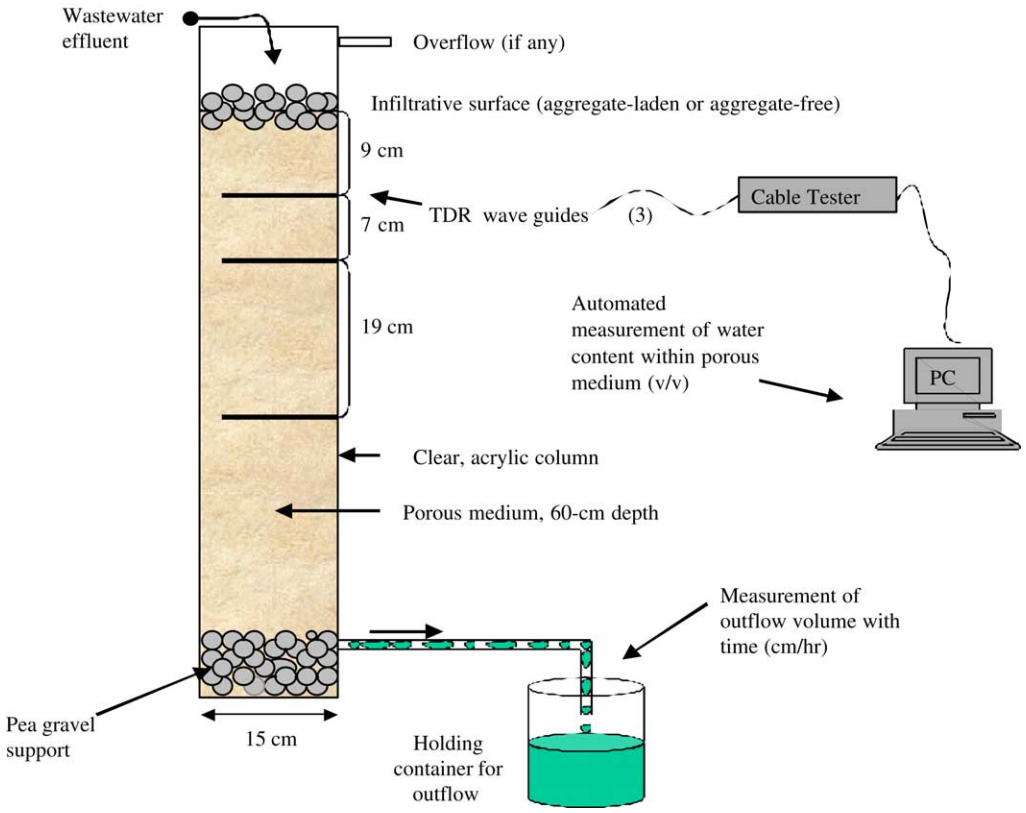

Fig. 1. Schematic of column set-up (TDR, time domain reflectometry).

The bonding of sand to the interior wall of the column was intended to roughen the sidewall and minimize preferential sidewall flow (Corwin, 2000). The columns were selected randomly for construction, packing, and grouping into loading regimes to negate any bias or pattern.

A 5 cm deep layer of washed pea gravel (1–2 cm in diameter) was placed in the bottom of each column for structural support and to minimize clogging of the outlet port. The gravel was flushed twice with tap water after placement to promote settling and compaction. Each column was then packed with moist sand (~5.5% water by weight, $d_{10}=0.22$ mm, $d_{60}=0.60$ mm, total organic carbon = 0.017 dry wt%) in 5 cm increments to a total sand depth of 60 cm. The same packing procedure was followed to ensure uniformity within and between columns (Beach, 2001).

To measure moisture content (θ), TDR sensors (Evett, 2000), 10 cm in length, were installed at soil depths of 9, 16, and 35 cm in each column. All TDR sensors were connected through multiplexers to a Tektronics 1502C cable tester that served as a data logger. The Dynamax TDR system was automated and controlled using a personal computer. The software and data logger were configured according to manufacturer's recommendations (Evett, 2000) to automatically acquire water content measurements for each TDR sensor every 2 h.

Wastewater was acquired as needed from the Mines Park test site at CSM (multifamily housing units) and transported to the laboratory where it was stored in an insulated 300-gallon polyethylene tank. All columns received wastewater from this holding tank. The 16 columns were operated for a period of 138 days. Hydraulic parameters, such as water content, wastewater ponding levels, and volume throughput (i.e. column effluent) were monitored daily for a period of 131 days. During this period, three bromide tracer tests were conducted. Final infiltration rates were measured just prior to ending the experiments. The initial design hydraulic loading rates were 200, 100, 50, and 25 cm/d for LR1, LR2, LR3, and LR4, respectively. Initial design rates could not be maintained constantly due to experimental factors such as sediment accumulation in delivering tubing and periodic pump malfunctions. Therefore, actual starting rates were 87–100% of the design rates. In addition, biomat genesis resulted in decreased hydraulic throughput rates over time. These phenomena will be described in detail later in the text.

Biomat development within the columns eventually led to wastewater ponding at the soil infiltrative surface. Ponding conditions developed in LR1 and LR2 after the first few weeks of operation and quickly reached the overflow ports at 20 cm, remaining there for the duration of the experiment. In LR3 and LR4, the level of ponding fluctuated significantly throughout column operation. In addition, during the tracer tests, bromide was not applied to LR3 and LR4 as a continuous pulse due to the STE application method (dosed four times per day, Table 1). The methods used to analyze the hydraulic performance of LR1 and LR2 are not warranted for the dosed loading regimes (LR3 and LR4). Therefore, further discussion of LR3 and LR4 is not included herein. An analysis of hydraulic behavior and treatment of all columns based on effluent throughput rates is forthcoming (Lowe et al., submitted for publication).

2.2. Monitoring and measurements

2.2.1. Hydraulic conductivity measurements from falling-head experiments

The effective hydraulic conductivity (K_e) (L/t) of LR1 and LR2 was measured using a falling head test prior to wastewater load and just before column shutdown and dismantlement. The term effective is used because the column eventually becomes a heterogeneous system, where the hydraulic conductivity is controlled by biomat development (see Section 3), as well as the degree of saturation below the infiltrative surface.

For measurements prior to wastewater loading, all columns were up-flow saturated over a period of 8 h and allowed to sit ponded overnight to ensure saturation and to reduce air entrapment. Reference locations for initial and final head (h) were specified randomly at each measurement repetition. Eq. (1), derived using Darcy's law (McWhorter and Sunada, 1977), was used to calculate K_e.

$$K_e = \frac{L_e}{\Delta t}\left(\ln\left(\frac{L_e + h_0}{L_e + h_1}\right)\right) \quad (1)$$

The term L_e is the length of sand through which the head loss is occurring; Δt is the change in time during

the head drop; h_0 is the initial height of ponded water (L), which equals the initial head at the top of the column; h_1 is the final ponded water height or final head (L). The equation assumes a zero pressure-head boundary at the end of the column. This assumption is valid because the outflow tubes at the bottom of each column were open to the atmosphere. Thus, for both initial and final falling head tests, the effective hydraulic conductivity, K_e, is calculated for the entire column, where $L_e = 60$ cm.

2.2.2. Bromide tracer tests

Three bromide tracer tests were completed in the columns of LR1 and LR2 during the course of the experiment, resulting in a total of 24 individual column tracer tests. Tracer test 1 was completed prior to wastewater loading, tracer test 2 was completed 2 weeks after the start of the wastewater application, and tracer test 3 was completed 6 weeks after the start of wastewater application. The tracer tests were used to estimate mean travel times under each loading regime. The concentration-versus-time plots, or breakthrough curves (BTC), provide information about travel times, dispersion within the columns, and heterogeneities that develop due to continued wastewater application.

Tracer test 1 was completed prior to wastewater loading. Tap water containing 500 mg-Br^-/L was applied to each column at the rate prescribed for that loading regime (refer to Table 1) for 103 h (4.3 days). Percolate (column effluent) was initially collected four times per day at 8 am, noon, 4 pm, and 8 pm. The frequency of percolate sample collection decreased after tracer input ceased and percolate concentrations approached the lower detection limit. The Br^- concentration in the percolate was analyzed using a combination ion-selective electrode for bromide (Cole-Parmer, 2001). A moment analysis was conducted to determine the mean travel time of the center of mass of bromide tracer in each column. The mean travel time is obtained from the corrected, normalized first temporal moment (Divine et al., 2004), assuming a constant input pulse concentration and varying percolate volumes with time (Eq. (2)).

$$T = \frac{\int_0^{V_f} Ct \, dV}{\int_0^{V_f} C \, dV} - 0.5T_0 \tag{2}$$

where T is the travel time (h), C is the concentration (mg/L) at time t, dV is the change in percolate volume, T_0 is the input pulse duration (h), and V_f is the total volume of percolate collected at the column effluent.

Two additional bromide tracer tests were conducted during Weeks 2 and 6 of column operation (tracer tests 2 and 3, respectively). The bromide T_0 for these two tracer tests was 3 days. As in tracer test 1, samples were initially collected at 8 am, noon, 4 pm and 8 pm. The frequency of sample collection decreased after the input ceased. Sampling continued until concentrations approached $\sim$10 mg-Br^-/L, with a sampling frequency of once per 24 h period.

At the time of tracer test 3 (6 weeks), many of the columns were continuously ponded with wastewater. The actual input concentrations into these (ponded) columns were unknown, as samples were mistakenly not collected from the ponded water after tracer addition. Based on the measured percolate peak concentrations for all columns, it was estimated that the effective concentration for these columns was approximately 1500 mg-Br^-/L. The uncertainty of the input concentration compromised our ability to compute a mass balance on the influent and effluent bromide mass. However, the travel time calculation is not influenced.

2.2.3. Hydraulic conductivity estimations from tracer travel times

It is assumed that variations in the hydraulic properties of the infiltrative surface are the main control on differences in travel times computed for each tracer test. In order to approximate the effective hydraulic conductivity of the columns, a simple Darcy's law calculation (Eq. (3)) was performed on the columns in LR1 and LR2.

$$q = \frac{l\theta_a}{t} = -K_e \frac{\Delta H}{\Delta l} \tag{3}$$

where q is flux (L/t), θ_a is the average water content within the column, t is the mean travel time computed from bromide tracer test data, K_e is the effective hydraulic conductivity (L/t), and $\Delta H/\Delta l$ is the total head loss across a length l. For all tracer tests, the length (Δl) is 60 cm and corresponds to the distance between the top of the biomat (infiltrative surface) and the gravel–sand interface at the bottom of the column. The ΔH is computing by subtracting the head at

the bottom of the column from the head at the infiltrative surface (i.e. the pond height). Pressure heads at the lower gravel–sand interface are zero as described previously.

After the first few weeks of operation, LR1 and LR2 experienced almost continuous wastewater ponding at the level of their overflow ports (~20 cm). The stable ponding levels provided a constant-head boundary condition at the top of the column. Pressure heads and ponding levels were changed to total head using a datum located at a depth of 60 cm (bottom of the column). This allowed for the total head loss and hydraulic gradient across the column to be determined.

Travel times through the columns ($L=60$ cm) were obtained from the temporal moment analysis conducted on bromide tracer test data collected at Weeks 2 and 6 of column operation. The water content (θ_a) was calculated for each tracer test period by averaging the water content of the biomat (assumed to be saturated) and the TDR-derived water contents measured at 9, 16, and 35 cm depths within the columns.

Ponding had not occurred in LR2 during tracer test 2 (Week 2), so the method could not be used. Only three ponding level observations were made for LR1 during tracer test 2. The computed K_e for LR1 is based on an average ponding level (ranging from 1.5 to 20 cm due to rapid increases in ponding levels) over the 3-day tracer test. Thus, there is more uncertainty for the values calculated during this tracer test than for those calculated from measurements made during tracer test 3 (Week 6) for which the pond levels in LR1 and LR2 columns was relatively constant at the overflow-port level.

2.2.4. Normalized hydraulic conductivity of the biomat

With continued wastewater application and biomat development, a layered system evolves, in which a low-conductivity biomat layer sits atop a high-conductivity subsoil. Like crusted soils, the biomat layer tends to be very thin (1–4 cm) in relation to the parent soil below. The exact thickness of the biomat was not known during column operation. Although color variation can be used to some extent as an indicator of biomat presence, anoxic conditions within or below the biomat can also create zones of dark or blacken soil. To avoid the uncertainty that would result from visual estimations of biomat thickness, a lumped or normalized hydraulic conductivity of the biomat was calculated. Eq. (4a) is derived from the basic solution for effective hydraulic conductivity in a two-layer system with flow perpendicular to the layers (Fetter, 2001).

$$\frac{K_e}{b_{sc}} = \frac{1}{\frac{b_{bm}}{K_{bm}} + \frac{b_{ss}}{K_{ss}}} \tag{4a}$$

where K_e is the measured effective hydraulic conductivity of the column (L/t), K_{bm} is the hydraulic conductivity of the biomat (L/t), K_{ss} is the hydraulic conductivity of the subsoil (L/t), and b_{sc}, b_{bm}, b_{ss} are the thickness of the soil column (60 cm), biomat, and subsoil, respectively (L). Note that $b_{sc}=b_{bm}+b_{ss}$. If one assumes that the thickness of the biomat is small in comparison to the thickness of the subsoil, the term b_{ss}/K_{ss} can be written as:

$$\frac{b_{ss}}{K_{ss}} = \frac{b_{sc}}{K_{ss}} - \frac{b_{bm}}{K_{ss}} \approx \frac{b_{sc}}{K_{ss}} \tag{4b}$$

This assumption is acceptable because the actual biomats in these studies were typically thinner than 1 cm, and usually thinner than 0.5 cm, based on physical inspection during column dismantlement after completion of the experiments (Van Cuyk, 2002). Thus, the biomat generally comprises less than 1% of the total column length. After rearranging to isolate K_{bm}/b_{bm}, Eq. (4a) then becomes:

$$\frac{K_{bm}}{b_{bm}} = \frac{1}{\frac{b_{sc}}{K_e} - \frac{b_{sc}}{K_{ss}}} \tag{4c}$$

Based on water content data, the subsoil in most columns was unsaturated during both the tracer and final falling head tests. Ausland (1998) conducted a hanging column experiment on the same sand media used in this research effort. The resulting water retention data were used in conjunction with the Van Genuchten (1980) relationship (Eqs. (5a)–(5c)) and measured water contents to estimate the unsaturated hydraulic conductivity of the subsoil (K_{ss}) during the time periods of interest.

$$K_{ss} = K_s \Theta^{1/2}[1-(1-\Theta^{+1/m})^m]^2 \tag{5a}$$

$$\Theta = (\theta - \theta_r)/(\theta_s - \theta_r) \tag{5b}$$

$$m = 1 - 1/n \tag{5c}$$

where θ is volumetric water content; θ_r is residual water content; θ_s is the saturated water content; Θ is the effective water content; and m, and n are empirical parameters related to the porous-media characteristics. The saturated water content, θ_s, was assigned a value equal to the measured effective porosity of 0.35 (Beach, 2001). A nonlinear least-squares fitting routine was used to optimize the Van Genuchten parameters; the following values were obtained: $m=0.74$, $n=3.9$ and $\theta_r=0.05$.

3. Results and discussion

3.1. Falling-head hydraulic conductivity measurements

Effective hydraulic conductivity values were determined using a falling-head test before wastewater application and at the end of the experiment (mature-biomat tests). The K_e values were calculated from experimental data using Eq. (1). Because the columns were saturated during the clean-water, falling-head tests, the initial K_e values are equal to the saturated hydraulic conductivity (K_{sat}) values for each column. The K_e values calculated for LR1 and LR2 are presented in Table 2.

The initial K_{sat} values varied between 704 and 1015 cm/d, with a mean value of 873 cm/d, a standard deviation of 89 cm/d, and a coefficient of variation equal to 10%. To determine if there was a statistically significant difference between columns before applying wastewater in various loading regimes, a t-test was performed on all possible pairs. Results indicate that there is no significant difference (at a 95% confidence level) in initial K_{sat} values between any combination of loading regimes. Therefore, the packing procedure was reproducible and all columns exhibited similar initial hydraulic properties before wastewater application.

At the end of the experiment (138 days), a falling head test was performed on the columns. During the test, the change in ponding height (head above the infiltrative surface) was recorded over time as the column was allowed to drain. Up to 29 individual head measurements were recorded per column. Infiltration rates based on the $\Delta h/\Delta t$ for each column were then determined from the average of the individual measurements. Due to the presence of

Table 2
Estimated effective and normalized biomat hydraulic conductivities for columns in loading regimes 1 and 2 based on falling head and bromide tracer test data

Column	K_e (cm/d)				K_{ss} (cm/d)			K_{bm}/b_{bm} (d^{-1})		
	Initial K_{sat}	Week 2[a]	Week 6[a]	Week 20[b]	Week 2[a]	Week 6[a]	Week 20[b]	Week 2[a]	Week 6[a]	Week 20[b]
1A	891	72.45	4.56	1.84	70.37	26.74	45.30	–[c]	0.09	0.03
1B	704	40.12	5.79	2.64	64.64	29.29	60.06	1.76	0.12	0.05
1C	798	31.68	8.17	2.92	71.20	56.08	58.94	0.95	0.16	0.05
1D	915	23.39	3.33	1.20	53.38	28.86	27.70	0.69	0.06	0.02
Avg.	827	41.91	5.46	2.15	64.90	35.24	48.00	1.14	0.11	0.04
CV	0.12	0.51	0.38	0.36	0.13	0.40	0.31	0.49	0.38	0.23
2A	941	–[d]	7.68	4.42	–[d]	189.07	250.19	–[d]	0.13	0.07
2B	723	–[d]	10.56	4.34	–[d]	139.44	237.26	–[d]	0.19	0.07
2C	863	–[d]	4.53	2.32	–[d]	51.49	31.51	–[d]	0.08	0.04
2D	879	–[d]	3.84	1.13	–[d]	32.83	23.83	–[d]	0.07	0.02
Avg.	851.5		6.65	3.05		103.21	135.70		0.12	0.05
CV	0.11		0.47	0.53		0.71	0.92		0.45	0.51

[a] Week 2 and 6 K_e and K_{bm}/b_{bm} are based on bromide tracer tests results.
[b] Week 20 K_e and K_{bm}/b_{bm} are based on falling head tests prior to column shutdown and dismantlement.
[c] Negative value because $K_{ss}>K_e$ (which is not possible) due to uncertainty in K_{ss} estimation.
[d] The lack of measurable ponding in columns 2A through 2D (LR2) during Week 2 precludes the calculation of K_e and K_{bm}/b_{bm}.

a biomat, ponded wastewater was present at the infiltrative surface for all LR1 and LR2 tests.

To provide insight into the source of variability of the falling head test results, a two-way analyses of variance with replication was completed ($\alpha = 0.05$). The total variance of the falling head data was decomposed into the variance associated with the factors, such as loading regime and infiltrative surface architecture, and their interactions (i.e. loading regime plus infiltrative surface architecture). Results show that while the loading regime (i.e. rate of wastewater application) had a negligible effect on the infiltration rate (3% of the total variance), the infiltrative surface architecture (gravel-free versus gravel-laden) significantly affected the infiltrative rate (64% of the total variance at a 97% confidence level).

A one-tailed Student *t*-test was then used to compare the mean falling head infiltration rate for all gravel-free columns in LR1 and LR2 to the rates for all aggregate-laden columns in LR1 and LR2. The standard error of the mean for each surface type was also determined (Alder and Roessler, 1977; Snedecor and Cochran, 1980). The gravel-free mean falling head infiltration rate was 4.75 cm/d (standard error of the mean = 0.54) compared to the gravel-laden mean falling head infiltration rate of 2.84 cm/d (standard error of the mean = 0.44). The *t*-test showed that the two means are different at 98% confidence level indicating that the gravel-free infiltration rate exceeds that of the gravel-laden columns. Further evaluation of the means using a two-tailed Student *t*-test revealed a significant difference in the mean gravel-free and gravel-laden falling head infiltration rates at a 96% confidence interval ($\alpha = 0.04$).

The K_e values for LR1 and LR2 at the end of column operation (20 weeks) were then calculated from falling head measurements using Eq. (1) (Table 2). The final K_e values varied between 1.13 and 4.42 cm/d, with a mean value of 2.6 cm/d, a standard deviation of 1.27 cm/d, and a coefficient of variation equal to 48.7%. The biomat formation caused a two-order of magnitude reduction in K_e during the 20-week experiment, and resulted in a slight increase in K_e variability among the columns in LR2 compared to initial K_{sat} values and K_e at 6 weeks.

Results of two-way analyses of variance with replication of the estimated K_e values at 6 and 20 weeks indicate trends similar to the observed falling head infiltration rate trends with more pronounced contributions observed due to loading regime and infiltrative surface architecture over time (17.4 and 43.0% of the total variance at 6 and 20 weeks, respectively, at 81 and 93% confidence levels). At 20 weeks, a one-tailed Student *t*-test reveals the gravel-free mean K_e (3.3 cm/d) is greater than the gravel-laden mean K_e (1.9 cm/d) at 93% confidence (ratio of the mean values, gravel-free/gravel-laden, is 1.75).

3.2. Water content distribution and unsaturated hydraulic conductivity

Based on simple analytical modeling by Buoma (1975) and numerical modeling by Beach and McCray (2003), biomat development causes unsaturated conditions in the subsoil below the biomat. Thus, the reduction in K_e may be due in part to unsaturated conditions (i.e. lowered relative permeability) as well as the reduced conductivity of the biomat (the biomat was at or near saturation throughout the experiment). These two factors are linked. Less permeable biomats yield lower overall flow rates and thus smaller subsoil water saturations, further reducing the effective hydraulic conductivity (Beach and McCray, 2003). Therefore, measured K_e's were used in conjunction with estimated unsaturated hydraulic conductivities of the subsoil (Table 2) to approximate the hydraulic resistance of the biomat zone (K_{bm}/b_{bm}). These results are discussed later in the paper.

Water content measurements below the biomat were relatively uniform within each column and generally varied between 45 and 75% of saturation during column operation (Table 3). The subsoil is unsaturated in all columns, therefore, one would expect some impact on the K_e (discussed in a subsequent section). A more detailed analysis of water content can be found in Beach (2001).

3.3. Bromide tracer tests: breakthrough curve analyses

Tracer tests were conducted on all columns. Figs. 2 and 3 show representative bromide BTCs from LR2 for one gravel-free and one gravel-laden column, respectively. BTCs for the other loading regimes were surprisingly similar. The presence of gravel appears to have negligible influence on the BTCs.

Table 3
TDR-derived water contents at Weeks 2, 6, and 20 of column operation

Column	Average water content		
	Week 2	Week 6	Week 20
1A	0.21	0.17	0.20
1B	0.21	0.18	0.21
1C	0.21	0.20	0.20
1D	0.19	0.17	0.16
Avg.	0.21	0.18	0.19
CV	0.05	0.09	0.12
2A	0.19	0.25	0.27
2B	0.21	0.25	0.28
2C	0.20	0.19	0.17
2D	0.20	0.18	0.16
Avg.	0.20	0.22	0.22
CV	0.04	0.19	0.29

The BTCs from tracer test 1 (clean water) were very similar for all columns, indicating that the hydraulic regimes prior to wastewater loading were similar. During the initial clean water loading (tracer test 1), bromide breakthrough occurs rather quickly (less than 10 h). For tracer test 1, the bromide BTCs show a decrease in concentrations after the peak concentration had occurred while bromide was still being applied to the columns. This change in bromide concentrations in the column effluent was due to a change in bromide concentration in the influent holding tank that occurred when refilling the tank. Note that this concentration fluctuation will not adversely influence the travel time calculation, which is based solely on effluent concentrations.

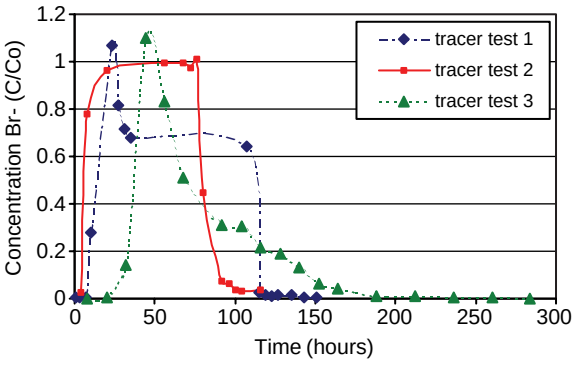

Fig. 2. Bromide breakthrough curves during tracer tests 1–3 for gravel-free column in LR2 (A).

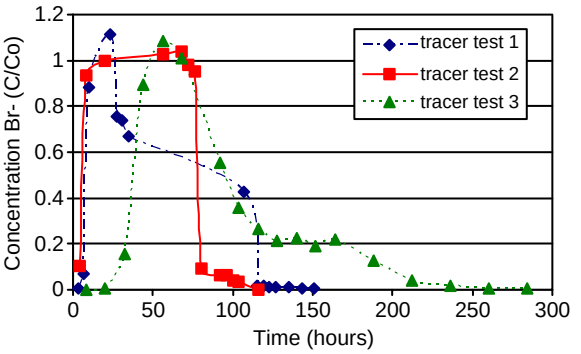

Fig. 3. Bromide breakthrough curves during tracer tests 1–3 for gravel-laden column in LR2 (D).

The secondary plateau of the BTC, corresponds to the concentration of bromide in the holding tank after the refilling and occurs at a C/C_0 value of about 0.7. Note that the latter portion of this plateau ends in a sharp decline to zero concentrations. This lack of tailing indicates that the porous medium in the columns is relatively homogeneous.

Figs. 2 and 3 indicate that bromide breakthrough for tracer test 2 is similar to that for tracer test 1. Because the second tracer test was initiated after only 2 weeks of wastewater application, it is expected that little or no noticeable change would occur between these two tests. The BTC for test 2 looks like the traditional BTC in a homogeneous medium, with very little spreading at the front or tail end of the curve. In Week 6, breakthrough occurs later in all columns and significant tailing is observed. These changes are attributed to the biomat development at the infiltrative surface. Bromide is retarded in the low-permeability biomat, increasing the time to observed breakthrough for the bromide pulse center of mass. This phenomenon also creates a heterogeneous system within the columns, wherein a low-permeability zone sits atop a high-permeability sand. In general, heterogeneities cause additional dispersion of the solute front and increased tailing of the BTC (Brusseau, 1994), which are evident in Figs. 2 and 3.

Mean travel times (center of mass travel times) were computed from BTC data using Eq. (2), as described previously, and are shown in Table 4. The travel times are similar for LR1 and LR2. In general, travel time increases with each successive tracer test.

Table 4
Computed mean travel times from bromide tracer tests

Column	Infiltrative surface architecture	Travel time (h)		
		Week 0	Week 2	Week 6
1A	Gravel-free	2.50[a]	3.65	39.70
1B		2.50[a]	6.26	34.24
Average			4.96	36.97
1C	Gravel-laden	2.50[a]	7.75	27.23
1D		2.50[a]	9.71	55.21
Average			8.73	41.22
2A	Gravel-free	10.61	9.99	36.00
2B		7.53	7.77	25.73
Average		9.07	8.88	30.87
2C	Gravel-laden	4.74	6.75	46.31
2D		5.10	7.69	49.17
Average		4.92	7.22	47.74

[a] Travel time is estimated, not computed, as described in text.

The most significant increase occurred between the second and third tracer test. During this time, continuous ponding developed in LR1 and LR2, indicative of biomat development and increased impedance to flow. The computed travel times for LR1 during tracer test 1 (Week 0) were negative and are attributed to the lack of sufficient sampling density (an imprecise solute mass definition) at early times. In LR1, peak bromide concentration occurred between the first (0.5 h) and second (4 h) sampling events. To allow comparison with later tracer tests, the mean travel times for LR1 during tracer test 1 were assumed to be 2.5 h, which is the time required to displace one pore volume of effluent wastewater.

3.4. Bromide tracer tests: hydraulic conductivity calculations

Table 4 summarizes the travel times used in Eq. (3) to calculate K_e values. The resulting K_e values are shown in Table 2. Based on the Darcy calculations, the K_e of the columns in LR1 decreased by an order of magnitude from Week 2 to 6. For all columns, a reduction of two orders of magnitude occurred between the K_e measured at system startup and the final measurements at Week 20. The average K_e values after Weeks 6 and 20 are similar for LR1 and LR2 with much of the reduction in K_e occurring over the first several weeks.

3.5. Evolution of hydraulic conductivity of the infiltration zone

The effective hydraulic conductivity (K_e) values for the columns decrease with time due to biomat formation. It is interesting to note that, relative to the initial K_{sat} values, the K_e values reach a similar value (between 1 and 5 cm/d) regardless of loading regime or infiltrative surface architecture. Although, it appears that the infiltrative zone is somewhat more conductive for the gravel-free surface, particularly in LR2.

The decrease is related to the total volume of wastewater applied and this practical relationship is discussed in more detail below. Fundamentally, the decrease in K_e is due to increased resistance to flow in the biomat zone for reasons described earlier, as well as development of unsaturated flow below the biomat. The unsaturated regime occurs because the biomat has a higher capillarity relative to the underlying subsoil, due to the smaller average pore-size of the biomat. This process leads to formation of a 'capillary break' that develops when a fine-grained soil overlies a coarser grained soil. Unsaturated hydraulic conductivities in the subsoil (K_{ss}) have the potential to be orders of magnitude lower than saturated hydraulic conductivities (K_{sat}).

The estimated K_{ss} values are shown in Table 2. It is worth noting that there is considerable uncertainty in these estimated values, which are obtained from the theoretical Mualem relationship that links measured capillary pressure versus soil moisture relationships to K_{ss}. This relationship is likely to have the most error at low water contents where the exact shape of the capillary curve (and thus the K_{ss} curve) is most uncertain. Because the $K_{ss}(\theta)$ function is highly nonlinear, small uncertainties in the capillary curve can translate into large uncertainties in the K_{ss} value. Nonetheless, this analysis provides useful insight into the relative effects of biomat formation and development on the unsaturated flow regime below the infiltrative surface.

Influences of unsaturated hydraulic conductivity can be analyzed by comparing the K_{ss} values in Table 2 to the K_{sat}, K_e, and K_{bm}/b_{bm} values. For the sake of discussion, the final K_{bm}/b_{bm} values can be transformed into approximate K values by multiplying by a representative biomat thickness. For this study,

the final biomat thickness ranged between 0.5 and 1.0 cm, based on physical inspection of the biomat zone after completion of the experiments assumed (Van Cuyk, 2002). Both the biomat and the unsaturated flow regime contribute significantly to reducing the overall K of the infiltrative surface. If one assumes a biomat thickness ranging between 0.5 and 1.0 cm, K_{bm} is generally about two orders of magnitude smaller than the final K_e values and three orders of magnitude smaller than final K_{ss} values. However, the biomat does not totally dominate the flow regime, as is evidenced by the fact that the final K_e numbers are similar to the K_{ss} values in many cases. If the biomat dominated the hydraulic conductivity of the system, then the long-term or final K_e would be similar to the K_{bm} at 20 weeks. Therefore, both the biomat and the formation of an unsaturated regime below the biomat contribute to the overall reduction of the infiltration rate. However, the two cannot be separated because the unsaturated regime occurs because of the biomat formation. As the biomat becomes less conductive, the soil below the layer also becomes less and less saturated, with decreasing K_{ss}.

3.6. Normalized hydraulic conductivity of the biomat zone

Normalized hydraulic conductivities of the biomat zone (K_{bm}/b_{bm}) in each column were estimated from calculated K_e and K_{ss} (Eqs. (4a)–(4c)). In both LR1 and LR2, the normalized conductivities of the biomat zone decrease with the length of column operation (Table 2). This reduction in K_{bm}/b_{nm} from Week 2 to 20 can be attributed to either a decrease in hydraulic conductivity of the biomat, an increase in biomat thickness, or both. According to the literature (Jones and Taylor, 1965; Thomas et al., 1966; Bouma, 1975; Siegrist and Boyle, 1987; Tyler et al., 1991; Tyler and Converse, 1994) biomat development results from both the accumulation of suspended solids within soil pores and microbial growth as a result of microbiological activity. Therefore, it seems reasonable to assume that a decrease in permeability due to pore filling, as well as increase in biomat thickness is contributing to the overall increase in hydraulic resistance of the biomat zone.

3.7. Effective hydraulic conductivity as a function of wastewater loading

Siegrist (1987) and Siegrist and Boyle (1987) suggested that the rate of biomat development and associated infiltration capacity loss are a function of the mass-loading rate of wastewater pollutants. Our results support this hypothesis. However, our results also indicate that, for a given soil type and STE, once the biomat matures to the point of continuous ponding, the resulting hydraulic conductivity of the biomat, as well as the effective hydraulic conductivity of the entire system may be somewhat independent of historical loading rates. In other words, two systems of the same soil type loaded under differing design rates may, over time, develop a similar hydraulic resistance. This probably occurs because the biomat forms relatively quickly and thereafter controls the long-term infiltration rate. However, the transient values of both K_e and K_{bm}/b_{bm} can be predicted from the cumulative volume of wastewater infiltrated into the PMB.

The relationship between both K_e and K_{bm}/b_{bm} and cumulative volume throughput (effluent) for LR1 and LR2 are shown in Figs. 4 and 5. Research related to crusted soils has lead to solutions for infiltration across crust-soil boundaries. Biomat development and its influence on infiltration rates in PMB is similar, in many ways, to the reduced conductivity and related

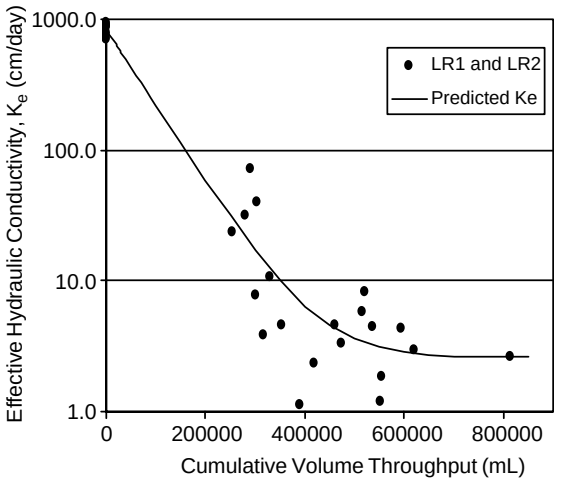

Fig. 4. Effective hydraulic conductivity as a function of cumulative volume throughput for loading regimes 1 and 2.

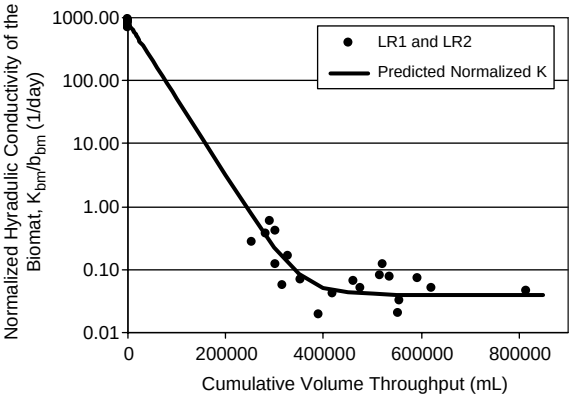

Fig. 5. Normalized hydraulic conductivity as a function of cumulative volume throughput for loading regimes 1 and 2.

soil-water processes found in crusted or sealed soils. A Horton-type hydraulic conductivity function can be used to simulate a developing biomat, where the biomat layer is very thin and assumed to be saturated from the beginning of the infiltrative process (Mualem and Assouline, 1992). Both K_e and K_{bm}/b_{bm} are approximated reasonably well using this type of exponential decay relationship (Eqs. (6a)–(6c)).

$$K(V) = K_f + (K_s - K_f)\, e^{-\chi V} \tag{6a}$$

$$K_e = 2.6 + 836.4\, e^{-1.35E-5V} \tag{6b}$$

$$\frac{K_{bm}}{b_{bm}} = 0.04 + 838.958\, e^{-2.80E-5V} \tag{6c}$$

where $K(V)$ is the hydraulic conductivity (L/t) of the system as a function of volume, V (L^3); K_f is the final hydraulic conductivity of the system (L/t); K_s is the initial saturated hydraulic conductivity of the system (L/t), and χ is a constant fitting parameter. Note that Eq. (6a) can be used for either K_e or K_{bm}/b_{bm}, where K_f is the final value for the respective K. K_s is taken as the average initial saturated hydraulic conductivity for LR1 and LR2. The final hydraulic conductivity (K_f) of the system is assumed to equal the average K_e or K_{bm}/b_{bm} at the end of system operation (Week 20). As with similar models (Mualem and Assouline, 1992), the biomat thickness is not explicitly specified. Instead, the biomat is assumed to act as a very thin, buffer between ponded conditions at the infiltrative surface and unsaturated subsoil below. The fitted values for the exponential models (Eqs. (6b) and (6c)) are shown on Figs. 4 and 5. Interestingly, the values for biomat conductance exhibit less scatter than those of effective K, even though the biomat values include the influences of estimated subsoil hydraulic conductivities. For general application, the biomat relationship is probably more useful, because these are likely to be similar for a variety of soil systems. The unsaturated hydraulic conductivities, however, are likely to vary greatly depending on subsoil type.

The greatest uncertainty between model and data fit appears to be early in system life, where the effective hydraulic conductivity of the infiltrative surface declines rapidly. Therefore, to improve predictive capabilities, measurement density should be increased during early time periods.

4. Conclusions

This research was performed to evaluate biomat genesis and the influence of biomat formation on the effective hydraulic conductivity (K_e) of the columns and the hydraulic conductance K_{bm}/b_{bm} of the biomat zone. The following conclusions are drawn:

1. The reduction in the K_e due to biomat formation is due to two factors: reduced hydraulic conductivity of the thin biomat, and a reduced hydraulic conductivity of the subsoil due to development of a biomat-induced unsaturated flow regime. If a biomat thickness of 0.5–1.0 cm is assumed, the resulting biomat hydraulic conductivity (K_{bm}) is three orders of magnitude smaller than the unsaturated hydraulic conductivity (K_{ss}). However, the relatively large thickness of the vadose zone causes the K_{ss} to be an important contributor to the overall K_e value.
2. K_{bm}/b_{bm} values calculated for the biomat region in the continuously loaded columns reached near steady values after less than 3 weeks of operation.
3. After 20 weeks of wastewater application, the K_e values for the infiltrative-surface zone were generally less than 1.0% of the values measured prior to wastewater application.
4. The computed normalized biomat hydraulic conductivity (K_{bm}/b_{bm}) values at the end of the 20-week experimental period are very similar.

The similarities in K_{bm}/b_{bm} suggest that for a given sand media, STE, and application method, an equivalent long-term biomat hydraulic resistance will be reached independent of hydraulic loading history.

5. A Horton-type exponential decay equation used previously for crusted soils may be used to relate K_e and K_{bm}/b_{bm} to the cumulative volume loading of wastewater.

Acknowledgements

This work was sponsored in part by Infiltrator Systems, Inc., and by the US Department of Education through a GAANN graduate-student fellowship to Ms Beach. The Alexander Deussen professorship in the Jackson School of Geosciences at The University of Texas at Austin supported manuscript preparation. Colorado School of Mines researchers John Albert, Sheila Van Cuyk, and Abigail Wren are acknowledged for their assistance with the laboratory experiments. The reviewers would also like to thank Dr Karen Salvage (State University of New York at Binghamton) and one anonymous reviewer for suggestions that significantly improved the manuscript.

References

Alder, H.L., Roessler, E.B., 1977. Introduction to Probability and Statistics, sixth ed. W.H. Freeman and Company, San Francisco, CA.

Ausland, G., Jenssen, P.D., Siegrist, R.L., Gudimov, A., 1998. Hydraulics and Purification in Wastewater. Doctoral Dissertation, Colorado School of Mines, Golden, CO.

Beach, D.N.H., 2001. The Use of One-dimensional Columns and Unsaturated Flow Modeling to Assess the Hydraulic Processes in Soil-Based Wastewater Treatment Systems. Master of Science Thesis, Colorado School of Mines, Golden, CO.

Beach, D.N.H., McCray, J.E., 2003. Numerical modeling of unsaturated flow in wastewater soil absorption systems. Ground Water Monitoring and Remediation 23 (2), 64–72.

Bouma, J., 1975. Unsaturated flow during soil treatment of septic tank effluent. ASCE, Journal of Environmental Engineering Division 101 (EE6), 967–983.

Brusseau, M.L., 1994. Transport of reactive contaminants in heterogeneous porous media. Reviews of Geophysics 32 (3), 285–313.

Cole-Parmer Instrument Company, 2001. Operating Instructions for Cole-Parmer 27502-04, -05 Bromide Electrodes, 1092.

Corwin, D.L., 2000. Evaluation of a simple lysimeter-design modification to minimize sidewall flow. Journal of Contaminant Hydrology 42, 35–49.

Divine, C.E., McCray, J.E., Wolf Martin, L.M., Blanford, W.J., Blitzer, D.J., Brusseau, M.L., Boving, T.B., 2004. Partitioning tracer tests as a remediation metric: case study at naval amphibious base little creek, Virginia beach, Virginia. Remediation Journal 14 (2), 7–31.

Evett, S.R., 2000. Time Domain Reflectometry (TDR) System Manual. Dynamax, Inc.

Fetter, C.W., 2001. Applied Hydrogeology, fourth ed. Prentice Hall, Upper Saddle River, NJ pp. 105–106.

Hargett, D.L., Tyler, E.J., Siegrist, R.L., 1981. Soil infiltration capacity as effected by septic tank effluent application strategies, On-Site Wastewater Treatment: Proceedings from the Third National Home Sewage Treatment Symposium. ASAE Publication, St Joseph, MI.

Jones, J.H., Taylor, G.S., 1965. Septic tank effluent percolation through sands under laboratory conditions. Soil Science 99 (5), 301–309.

Keys, J.R., Tyler, E.J., Converse, J.C., 1998. Predicting life for wastewater absorption systems, On-Site Wastewater Treatment: Proceedings of the Eighth National Symposium on Individual and Small Community Sewage Systems. ASAE Publication, St Joseph, MI pp. 3–98, see also pages 167–176.

Lowe, K.S., Huntzinger-Beach, D.N., Van Cuyk, S.M., Siegrist, R.L., McCray, J.E., submitted for publication. Performance evaluation of wastewater renovation by sandy porous media-biofilters. Journal of Environmental Engineering.

McWhorter, D.B., Sundada, D.K., 1977. Ground-water Hydrology and Hydraulics. Water Resources Publications, Fort Collins, CO. 290 p.

Mualem, Y., Assouline, S., 1992. Flow processes in sealing soils: conceptions and solutions. In: Sumner, M.E., Stewart, B.A. (Eds.), Soil Crusting: Chemical and Physical Processes. Lewis Publishers, Boca Raton, FL, pp. 128–129.

Schwager, A., Boller, M., 1997. Transport phenomena in intermittent filters. Water Sciences Technology 35 (6), 13–20.

Siegrist, R.L., 1987. Soil clogging during subsurface wastewater infiltration as affected by effluent composition and loading rate. Journal of Environmental Quality 16 (2), 181–187.

Siegrist, R.L., Boyle, W.C., 1987. Wastewater induced soil clogging development. Journal of Environmental Engineering 113 (3), 550–566.

Siegrist, R.L., Tyler, E.J., Jenssen, P.D., 2001. design and performance of onsite wastewater soil absorption systems. Invited White Paper Presented at the National Research Needs Conference Proceedings: Risk-Based Decision Making for Onsite Wastewater Treatment. EPRI Report No. 1001446, Electric Power Research Institute, Palo Alto, CA.

Snedecor, G.W., Cochran, W.G., 1980. Statistical Methods, seventh ed. Iowa State University Press.

Thomas, R.E., Schwartz, W.A., Bendixen, T.W., 1966. Soil chemical changes and infiltration rate reduction under sewage

spreading. Soil Science Society of America Proceedings 30, 641–646.

Tyler, E.J., Converse, J.C., 1994. Soil acceptance of onsite wastewater as affected by soil morphology and wastewater quality, On-Site Wastewater Treatment: Proceedings of the Seventh National Symposium on Individual and Small Community Sewage Systems. ASAE Publication, St Joseph, MI pp. 18–94, see also pages 185–194.

Tyler, E.J., Milner, M., Converse, J.C., 1991. Wastewater infiltration from chamber and gravel systems, On-Site Wastewater Treatment: Proceedings of the Seventh National Symposium on Individual and Small Community Sewage Systems. ASAE Publication, St Joseph, MI pp. 10–91, see also pages 214–222.

Van Cuyk, S.M., 2002. Fate of Virus during Wastewater Renovation in Soil Porous Media Biofilters. PhD Disseration (T-5739), Colorado School of Mines, Golden, CO.

Van Cuyk, S., Siegrist, R., Logan, A., Masson, S., Fischer, E., Figueroa, L., 2001. Hydraulic and purification behaviors and their interactions during wastewater treatment in soil infiltration systems. Water Research 35 (4), 593–964.

Van Genuchten, M.Th., 1980. A closed-form equation for predicting the hydraulic conductivity of unsaturated soil. Soil Science Society America Journal 44, 892–898.